Talanta 164 (2017) 209–215

Contents lists available at ScienceDirect

Talanta

journal homepage: www.elsevier.com/locate/talanta

Selective nano-sensing approach for the determination of inorganic phosphate in human urine samples

Alaa A. Fadhel, Madeleine Johnson, Khang Trieu, Eda Koculi, Andres D. Campiglia*

Department of Chemistry, University of Central Florida, P. O. Box 25000, Orlando, FL 32816-2366, United States

ARTICLE INFO

Keywords:
Phosphate ions
Urine analysis
FRET
Lifetime analysis
Lanthanide sensor
Gold nanoparticles

ABSTRACT

A novel sensing approach is presented for the analysis of phosphate ions in human urine samples. The new sensor is based on the fluorescence energy transfer between a luminescent probe ($[Tb\text{-}EDTA]^{-1}$) and gold nanoparticles capped with a cetyltrimethylammonium bromide (Au NPs-CTAB). The strong affinity between CTAB receptors and phosphate ions results in a highly selective assay with minimum sample preparation steps. Possible chemical interference is monitored on real-time basis via luminescence lifetime analysis. The simplicity of analysis and the competitive limit of detection in the micro-molar concentration range provide a well-suited approach for routine monitoring of phosphate ions in numerous urine samples.

1. Introduction

Determination of inorganic phosphorous in human urine plays an important role in clinical diagnosis of various anomalies, including bone, kidney or glandular diseases as well as alcoholism or vitamin deficiency [1–4]. Clinical analysis of inorganic phosphorous in urine samples is often based on a modification of the UV–VIS absorption method developed by Daly and Ertingshausen [5] in which inorganic phosphate reacts with Molybdate to form a heteropolyacid complex. By measuring the absorbance of the complex at 340/380 nm, it is possible to determine inorganic phosphorous at the mM (10^{-3}M) concentration level. Lower concentration levels (10^{-6}M – 10^{-4}M) can be reached with a variety of analytical approaches [6], including photometric [7], spectrophotometric [8] and ion chromatographic [9] methods, fluorimetric [10] assays and bio-sensing approaches coupled to either amperometric [11] or fluorescence [12] detection modes. In this study, we introduce a nano-sensing approach for the accurate determination of μM (10^{-6}M) inorganic phosphorous in urine with minimum sample preparation steps.

Fig. 1 illustrates the concept of the present sensor, which is based on Fluorescence Resonance Energy Transfer (FRET). This technique is often used in biochemistry and structural biology to study macromolecular complexes of DNA, RNA, and proteins [13–15]. FRET involves a mechanism in which the energy of the emitting donor is transferred via non-radiative dipole-dipole interactions to an acceptor. Within a 10–100 Å range, the efficiency of FRET is inversely proportional to the sixth power of the distance (R^{-6}) between the donor (fluorophore) and the acceptor (quencher). During the process of energy transfer, the proximity between the donor and the acceptor reduces the quantum yield of the donor's emission. When the distance increases, the intensity of emission is restored effectively.

The luminescence donor chosen for these studies is the terbium-ethylenediaminetetraacetic acid complex ($[Tb\text{-}EDTA]^{-1}$). The long-lived luminescence of the lanthanide ion, which occurs in the milliseconds time domain, makes possible to time-discriminate against short-lived background fluorescence and scattered excitation light with rather simple, off-the-shelve, commercial instrumentation. Since the lanthanide ion emission results from shielded electronic transitions within the f-orbital manifold, the luminescence intensity of Tb^{3+} is less susceptible to oxygen quenching than traditional fluorescent dyes [16–22].

Gold nanoparticles (Au NPs) capped with cetyltrimethylammonium bromide (CTAB) play the role of the acceptor. CTAB is an amine based cationic quaternary surfactant often used to avoid aggregation of Au NPs in aqueous solution via electrostatic repulsion. The strong chemical affinity of CTAB molecules for phosphate ions makes them highly selective receptors in the presence of other inorganic ions [23–25]. The hydrophilic and electrostatic interactions between $[Tb\text{-}EDTA]^{-1}$ ions and the positive CTAB charges on the surface of Au NPs provide the close proximity between donor and acceptor for FRET to occur and quench the luminescence of $[Tb\text{-}EDTA]^{-1}$ (sensor off). The strong affinity that exists among phosphate ions and CTAB displaces $[Tb\text{-}EDTA]^{-1}$ from the proximities of Au NPs to the extent that FRET does no longer occur (sensor on).

Although individual elements of our approach have been anticipated previously, the optimal combination of these features had not

* Corresponding author.
E-mail address: andres.campiglia@ucf.edu (A.D. Campiglia).

http://dx.doi.org/10.1016/j.talanta.2016.11.017
Received 9 August 2016; Received in revised form 3 November 2016; Accepted 4 November 2016
Available online 12 November 2016
0039-9140/ © 2016 Elsevier B.V. All rights reserved.

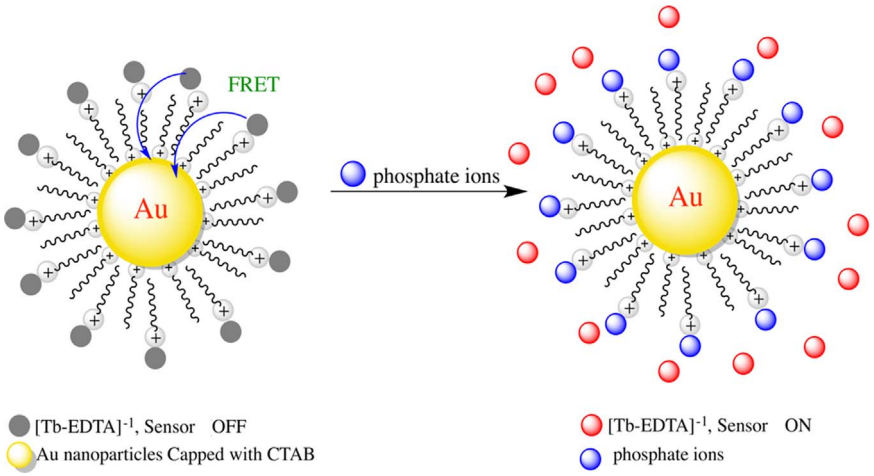

Fig. 1. Schematic diagram illustrating the principle of the proposed sensor.

been realized for their practical and straightforward implementation. The main significant aspect of our proposition is the way we have integrated all these features together. The direct determination of phosphate ions at micro-molar concentrations is possible with no need of sample pre-concentration steps. Sample preparation consists of a two-cycle urine filtration step followed by a 10 min urine-sensor mixing step. Considering the possibility to mix simultaneously numerous samples with different aliquots of the sensing solution, total analysis time is practically reduced to the measuring step in the spectrofluorimeter. Quantitative analysis based on a total of four standard additions takes no longer than 5 min per sample. Assuming that ten urine samples are mixed in parallel with ten aliquots of sensing solution, total analysis time takes less than 10 min per sample.

2. Experimental

2.1. Chemicals and reagents

All the reagents and solvents were purchased at their highest available purity and used without further purification. Chloroauric acid, sodium borohydride, CTAB, trisodium phosphate (Na_3PO_4), sodium acetate, sodium fluoride, and sodium sulfite were obtained from Aldrich. Sodium carbonate, urea, creatinine, sodium nitrate, sodium hydroxide, and sodium iodide were obtained from Alfa-Aesar. HEPES buffer (pH ≈7.4) was acquired from Acros Organics. Ascorbic acid was purchased from Fisher. Nanopure water from a Barnstead Nanopure Infinity water purifier was used throughout.

2.2. Synthesis of gold nanoparticles capped with CTAB

The synthesis of Au NPs followed the method previously reported by Nikoobakht and El-Sayed [26]. A seed solution was prepared by mixing aqueous CTAB (2 mL, 1.0 mol L^{-1}) with $HAuCL_4$ (18 μL, 0.029 mol L^{-1}). In order to avoid CTAB precipitation, the solution was heated to approximately 35 °C and gently stirred. Ice cold $NaBH_4$ (120 μL, 0.010 mol L^{-1}) was then added to the mixture causing the color to turn murky brown. Prior to use, the seed solution was allowed to mix for ½ hour.

Growth solutions were prepared in 10 mL beakers by mixing CTAB (10 mL, 1.0 mol L^{-1}) with $HAuCL_4$ (180 μL, 0.029 mol L^{-1}). The growth solutions were mixed and heated to about 35 °C to avoid CTAB precipitation as before. Ascorbic Acid (70 μL, 0.0788 mol L^{-1}) was then added to the growth solution causing it to change colors from yellow to clear. The seed solution (35 μL) was then transferred to the growth solution, stirred for 5 s, and allowed to sit for 30 min undisturbed. During this time the growth solution changed colors from clear to deep purple. After 30 min the solutions were removed from the heat source and kept at room temperature until further use.

2.3. Characterization of gold nanoparticles

The particle size distribution of Au NPs was obtained via light scattering with a Zetasizer Nano ZS9 instrument purchased from Malvern. UV–Vis absorption spectra of Au NPs were recorded with a Cary 50 spectrophotometer equipped with a 75 W pulsed Xenon lamp (spectral radiance of 190–1100 nm), a monochromator (fixed optical band-pass of 1.5 nm), a beam-splitter and two silicon photo-diode detectors.

2.4. Preparation of the $[Tb\text{-}EDTA]^{-1}$ probe

Stock solutions of 10^{-3} mol L^{-1} Tb^{3+} and 10^{-3} mol L^{-1} $EDTA^{-4}$ were prepared in HEPES buffer (pH ≈7.4). Stock solutions were mixed at the following Tb^{3+}: $EDTA^{-1}$ concentration ratios: 1:0, 1:0.25, 1:0.5, 1:1 and 1:1.5. Mixtures were shaken for 5 min prior to luminescence measurements. The Tb^{3+}-$EDTA^{4-}$ mixture with the highest luminescence signal was then diluted with HEPES buffer to reach final Tb^{3+} concentrations equal to 10^{-4}, 10^{-5} and 10^{-6} mol L^{-1}.

2.5. Sensing solution

350 μL of Au NPs-CTAB stock solution (optical density =0.74 OD) were added to 50 μL of a 10^{-4} mol L^{-1} $[Tb\text{-}EDTA]^{-1}$ solution and 100 μL of water. After 10 min of mechanical shaking, the mixture was ready to use for phosphate sensing.

2.6. Luminescence measurements

Luminescence intensities, excitation and emission spectra were recorded with a commercial spectrofluorimeter (FluoroMax-P from Horiba Jobin-Yvon) equipped with a continuous 100 W pulsed xenon lamp with broadband illumination from 200 to 1100 nm. The excitation and emission monochromators had the same reciprocal linear dispersion (4.2 nm mm^{-1}) and accuracy (± 0.5 nm with 0.3 nm resolution). Both diffraction gratings had the same number of grooves per unit length (1200 grooves·mm^{-1}) and were blazed at 330 nm (excitation) and 500 nm (emission). A photomultiplier tube (Hamamatsu, model R928) with spectral response from 185 to 650 nm was used for fluorescence detection operating at room temperature in the photon-counting mode. Commercial software (DataMax) was used to computer-control the instrument. Measurements were made by pouring undegassed liquid solutions into micro-quartz cuvettes (1 cm path length

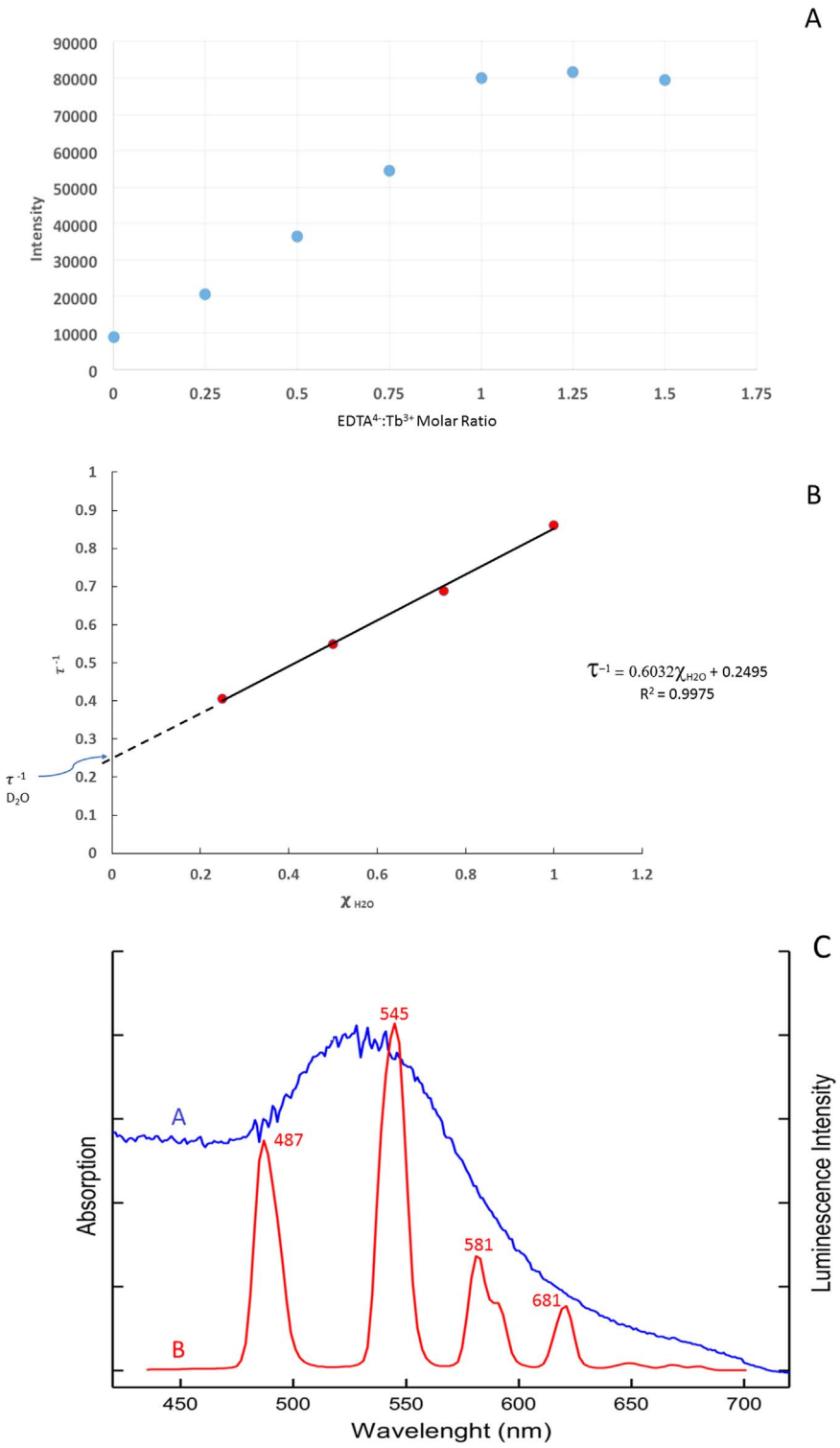

Fig. 2. (A) Luminescence intensity in counts.s^{-1} of 10^{-5}M Tb^{3+} as a function of $EDTA^{4-}/Tb^{3+}$ molar ratio in HEPES buffer (pH≈7.5). Luminescence intensity measurements were made at $\lambda_{exc}/\lambda_{em}$ =240/545 nm using a 15/5 nm excitation/emission band-pass, 20 excitation pulses and 0.010/9 ms delay/gate times; (B) Reciprocal luminescence lifetime (τ^{-1}) in ms^{-1} of 10^{-5} M [Tb-EDTA]$^{-1}$ as a function of mole fraction of water (χ_{H2O}) in D_2O-H_2O mixtures in HEPES buffer (pH≈7.5).). Luminescence lifetime measurements were made at $\lambda_{exc}/\lambda_{em}$ =240/545 nm using a 15/5 nm excitation/emission band-pass and 20 excitation pulses per data point; (C) Absorption (blue trace, intensity in arbitrary units) and luminescence (red trace, intensity in counts.s^{-1}) spectra of Au NPs-CTAB and 10^{-5}M [Tb-EDTA]$^{-1}$in HEPES buffer (pH≈7.5). Luminescence and absorption intensities are not to scale. Luminescence intensity measurements were made at $\lambda_{exc}/\lambda_{em}$ =240/545 nm using a 15/5 nm excitation/emission band-pass, 20 excitation pulses and 0.010/9 ms delay/gate times.

× 2 mm width) that held a maximum volume of 400 µL. Luminescence emission was collected at 90° from excitation using appropriate cutoff filters to reject straight-light and second order emission.

2.7. Urine analysis

Human urine samples were prepared following a previously reported procedure [25] and used within one hour of sample collection. After two filtration cycles with filter paper Whatman #50, the con-

Table 1
Statistical comparison of luminescence intensities and lifetimes of the proposed sensor in the absence and the presence of potential interference.

Chemical species[a]	Luminescence intensity (cps)[b]	t_{exp}[c]	Luminescence lifetime (μsec)[d]	t_{exp}[e]
Control	367.0 ± 17.2	–	1060.3 ± 33.9	–
NO_3^-	330.3 ± 8.4	0.802	1101.7 ± 53.3	2.109
CH_3COO^-	349.3 ± 4.9	0.601	1164.0 ± 70.4	5.261
OH^-	367.3 ± 9.7	1.925	1099.3 ± 28.7	1.993
NO_2^-	283.6 ± 8.1	4.246	894.0 ± 15.5	8.426
I^-	210.3 ± 14.5	9.590	1100.3 ± 158.8	0.065
CO_3^{2-}	370.0 ± 7.8	2.125	1158.0 ± 44.8	4.999
Cl^-	380.7 ± 3.5	9.346	1145.0 ± 52.7	4.320
F^-	284.7 ± 21.4	4.095	1050.0 ± 90.0	0.517
Creatinine	218.7 ± 11.7	9.012	1074.3 ± 103.7	0.004
Urea	354.7 ± 6.8	0.994	1111.7 ± 73.6	2.612

[a] Control refers to 350 μL of Au NPs-CTAB stock solution (optical density =0.74 OD), 50 μL of a 10^{-4} mol L^{-1} [Tb-EDTA]$^{-1}$ solution and 100 μL of water. Concentrations of NO_3^-, CH_3COO^-, NO_2^-, OH^-, CO_3^{-2}, I^-, Cl^-, F^- and creatinine were 10^{-4} mol L^{-1}; concentration of urea was 10^{-3} mol L^{-1}.

[b] Luminescence intensities are the averages of three individual measurements made from three aliquots. All measurements were made at 240 nm (excitation) and 545 nm (emission), 20 excitation pulses per data point, a 15/5 nm excitation/emission band-pass, and delay and gate times of 0.01 and 9 ms, respectively.

[c] t_{exp} = experimental value of t calculated from the average intensities in column 2. t_{exp} values were calculated according to ref. [30]. Statistical equivalence corresponds to $t_{exp} \leq t_{crit} = 2.021$.

[d] Luminescence lifetimes are the averages of three individual measurements of three aliquots. All measurements were made at 240 nm (excitation) and 545 nm (emission) and 15/5 nm excitation/emission band-pass.

[e] t_{exp} = experimental value of t calculated from the average lifetimes in column 4. t_{exp} values were calculated according to ref. [30]. Statistical equivalence corresponds to $t_{exp} \leq t_{crit} = 3.182$.

centration of phosphate ions in each sample was determined via the multiple standard addition method.

3. Results and discussion

3.1. Synthesis of gold nanoparticles

The volumes of Ascorbic acid and seed solution used for the synthesis of Au NPs were optimized by monitoring the intensity and the position of the maximum wavelength of the surface Plasmon resonance (SPR) absorption band at 541 nm. This maximum wavelength is consistent with an average mean NP size approximately equal to 25 nm [28]. The signal intensity reached a maximum value with 70 μL of Ascorbic acid and 30 μL of seed solution. Upon addition of Ascorbic acid volumes ≥ 70 μL, the mixture changed colors from yellow to colorless indicating that the growth solution had been completely reduced. Volumes of Ascorbic acid lower than 70 μL caused the mixture to remain yellow indicating that the growth solution was not fully reduced. Volumes of seed solution lower than 30 μL yielded nanoparticles with the desired dimensions – i.e. SPR maximum wavelength ~ 541 nm - but at with lower concentrations than the optimum concentration with maximum signal intensity. Volumes of seed solution higher than 30 μL created smaller spheres that did not absorb at the desired wavelength range. The excess of CTAB and reactants was removed from the final solution via three centrifugation cycles at 13,000 rpm for 30 min centrifugation.

3.2. Luminescence probe for analytical use

Phosphate ions are only detected upon releasing of [Tb-EDTA]$^{-1}$ into the sample matrix (see Fig. 1). Therefore, the capability of sensing of low concentrations of phosphate ions depends on our ability to measuring luminescence signals from low concentrations of Tb^{3+} in urine samples. In aqueous media, the luminescence signal of Tb^{3+} is rather low due to chemical bonding with water molecules. Upon coordination of O-H groups from water molecules, efficient non-radiative deactivation of the excited $^5D_4$ level of Tb^{3+} takes place via weak vibronic coupling with the vibrational states of the O-H oscillators. Since the O-H oscillators act independently, the overall effect on the rate of radiation-less deactivation is proportional to the number of O-H oscillators in the inner coordination sphere of Tb^{3+} [29]. One possible way to enhance the luminescence of Tb^{3+} is to promote chemical interaction with a chelating agent capable to remove water molecules from its coordination sphere. If the O-H oscillators of the water molecules are replaced by lower frequency oscillators present in the chelating agent, the vibronic deactivation pathway becomes much less efficient. As a result, the luminescence signal of Tb^{3+} is enhanced, and the lifetime of its excited state becomes longer [29]. Tb^{3+} probes with rather long luminescence lifetimes are a good match to time-resolved techniques, which discriminate against short lived background fluorescence and scattered excitation light.

Upon interaction with $EDTA^{-4}$, the maximum luminescence signal of Tb^{3+} is obtained at a 1:1 $EDTA^{-4}$:Tb^{3+} molar ratio (see Fig. 2A). The plot in Fig. 2B shows the effect of H_2O and D_2O in the luminescence lifetime of [Tb-EDTA]$^{-1}$. Lifetime experiments were carried out with [Tb-EDTA]$^{-1}$ solutions prepared in aqueous buffer (HEPES) or in aqueous buffer:D_2O mixtures containing different volume ratios of H_2O-D_2O. Comparison of the experimental lifetime in aqueous buffer (τ_{H2O} =1.163 ± 0.0031 ms, n =3; χ_{H2O} =1) to the extrapolated lifetime value in pure D_2O (τ_{D2O} =4.008 ms) shows the effect of the replacement of O-H oscillators by the lower frequency O-D oscillators on the coordination sphere of Tb^{3+}. The number of water molecules (q) bound to Tb^{3+} in the [Tb-EDTA]$^{-1}$ complex was determined with the equation $q = A_{LN}(\tau^{-1}_{H2O} - \tau^{-1}_{D2O})$, where A_{LN} is the proportionality constant (A_{Tb} =4.2) for Tb^{3+} [29]. Since Tb^{3+} can accommodate up to eight or nine molecules of water in its first coordination sphere, the calculated value of q (2.56) value is in good agreement with the fact that EDTA coordinates to 6 sites in the first coordination sphere of Tb^{3+}. Optimization of instrumental parameters for best signal-to-background ratio resulted in 20 excitation pulses per data point, a 15/5 nm excitation/emission band-pass, and delay and gate times of 0.01 and 9 ms, respectively. Upon excitation at 240 nm, a 10^{-5} mol L^{-1} [Tb-EDTA]$^{-1}$ solution provides an acceptable spectral signature for analytical use. As shown in Fig. 2C, there is strong overlapping between the SPR absorption band of Au NPs-CTAB and the luminescence spectrum of [Tb-EDTA]$^{-1}$. This is an essential condition to promote FRET between the donor (lanthanide complex) and the acceptor (nanoparticles).

3.3. Probe displacement time

The interaction between phosphate ions and CTAB displaces [Tb-EDTA]$^{-1}$ from the proximities of Au NPs to the extent that FRET does no longer occur. As a result, the luminescence signal of the probe (donor) increases. For a 10^{-5} mol L^{-1} [Tb-EDTA]$^{-1}$ solution and within the concentration range of phosphate ions tested (25 –750 μmol L^{-1}), the time it took to reach the maximum signal depended on the concentration of phosphate ions. The longest time (≈6 min) and the shortest (≈3 min) times were observed with the 20 μmol L^{-1} and 750 μmol L^{-1} phosphate solutions, respectively. In order to provide enough time for the complete displacement of [Tb-EDTA]$^{-1}$, all further measurements were made after 10 min of shaking time at 1,200 rpm.

3.4. Analytical figures of merit

The reproducibility of the reference signal – i.e., the luminescence signal of the Au NPs-CTAB and [Tb-EDTA]$^{-1}$ mixture in the absence of phosphate ions - depends on its intensity. Within the range of concentrations tested (10^{-7} mol L^{-1} – 10^{-3} mol L^{-1}), the 10^{-5} mol L^{-1} [Tb-EDTA]$^{-1}$ solution was able to detect low phosphate concentrations and still provide a reproducible luminescence signal with relative

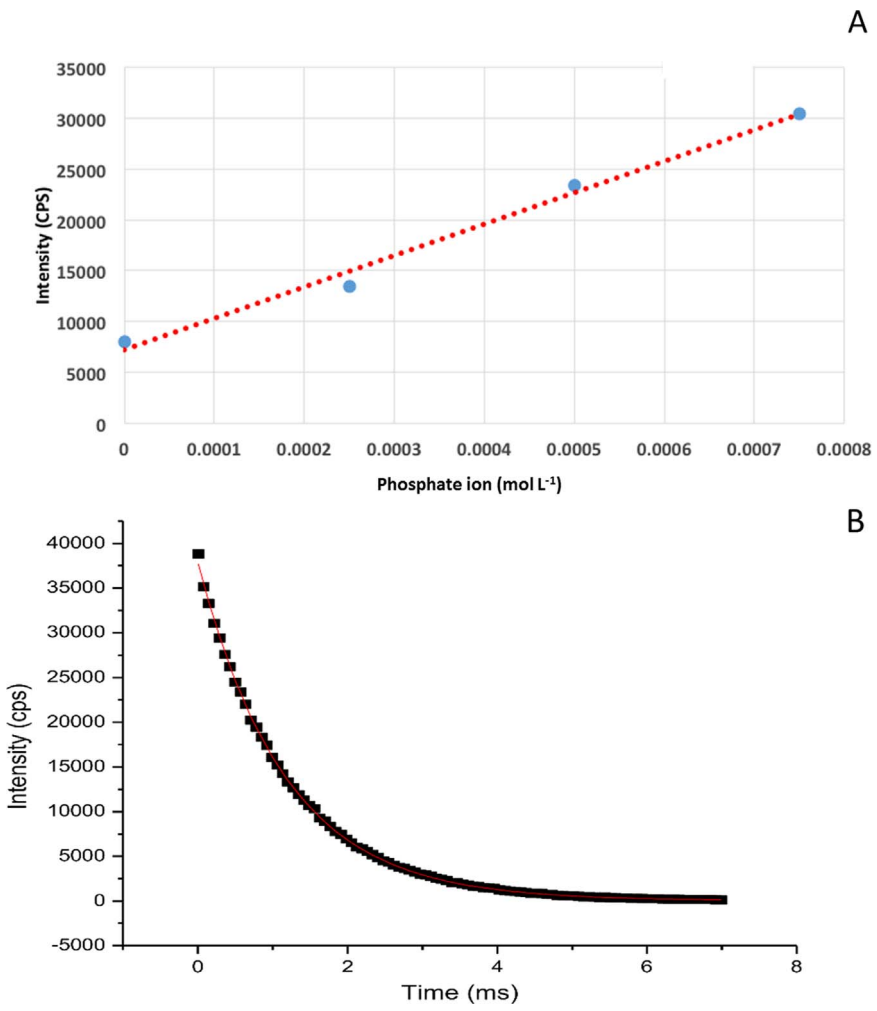

Fig. 3. (A) Calibration curve built with external standards of phosphate ions containing a synthetic mixture of the following species: NO_3^-, CH_3COO^-, NO_2^-, OH^-, CO_3^{-2}, I^-, Cl^-. F^-, urea and creatinine. With the exception of urea (10^{-3} mol L^{-1}), the concentration of all the other species was 10^{-4} mol L^{-1}. All luminescence measurements were made at $\lambda_{exc}/\lambda_{em}$ =240/545 nm using a 15/5 nm excitation/emission band-pass, 20 excitation pulses and 0.010/9 ms delay/gate times. (B) Fitted luminescence decay curve of the proposed sensor in the absence of synthetic mixture. All measurements were made in HEPES buffer (pH ~7.5) at $\lambda_{exc}/\lambda_{em}$ =240/545 nm using a 15/5 nm excitation/emission band-pass.

standard deviations lower than 5%. A calibration curve was then built with external standards consisting of pure phosphate solutions prepared in HEPES buffer (pH≈7.5). Microliter volumes of each phosphate standard were mixed with 350 µL of Au NPs-CTAB stock solution (optical density =0.74 OD) and 50 µL of a 10^{-4} mol L^{-1} [Tb-EDTA]$^{-1}$ solution and 100 mL of water. Luminescence measurements were made after 10 min of mechanical shaking at the maximum excitation (240 nm) and emission (545 nm) wavelengths of [Tb-EDTA]$^{-1}$. All intensities were measured after 20 excitation pulses using a 0.01 and 9 ms delay and gate times, respectively. The lowest concentration of the linear dynamic range of the calibration curve (11.7 – 750 µmol L^{-1}) corresponded to the limit of quantitation (LOQ). The LOQ was calculated according to the equation LOQ =10 s_R/m; where s_R was the standard deviation of the reference signal and m is the slope of the linear plot calculated via the least squares method [30]. A correlation coefficient close to unity (r =0.9994) demonstrated a satisfactory degree of linear association between phosphate concentration and luminescence signal. The limit of detection (LOD =3.8 µmol L^{-1}) was calculated as 3 s_R/m. Although a straightforward comparison with reported LODs [7–12] is difficult because different instrumental setups, experimental and mathematical approaches were used for their calculation, we can safely state that our LOD is of the same order of magnitude as those reported previously. The excellent reproducibility of measurements is demonstrated by the outstanding relative standard deviations within the LDR of the calibration curve.

3.5. Interference studies

The potential for matrix interference was first investigated by comparing the response of the sensor – i.e., 350 µL of Au NPs-CTAB (optical density =0.74 OD) and 50 µL of 10^{-4} mol L^{-1} [Tb-EDTA]$^{-1}$ and 100 µL of water - in the absence (control) and the presence of chemical species common to urine samples. These included NO_3^-, CH_3COO^-, NO_2^-, OH^-, CO_3^{-2}, I^-, Cl^-. F^-, urea and creatinine. Their concentrations were adjusted to previously reported values found in human urine samples [31–36]. The obtained results are summarized in Table 1.

The comparison of the luminescence signal recorded from the control in the absence and the presence of NO_3^-, CH_3COO^-, OH^- and urea reveals statistically equivalent intensities. This fact is an indication that these species do not release significant amounts of [Tb-EDTA]$^{-1}$ into the bulk of the sensing solution. This is probably due to a low chemical affinity between NO_3^-, CH_3COO^-, OH^- or urea with the CTAB receptors on the surface of Au NPs. Quenching of the sensor signal was observed in the presence of I^-, creatinine and NO_2^-. The quenching effect of I^- and creatinine can be attributed to inner filter effects caused by the strong absorption of these species in the excitation region of the probe (200 – 300 nm). Since the inner filter effect is not related to the chemical interaction between [Tb-EDTA]$^{-1}$ and the potential interference, there is no significant chance in the lifetime of the sensor. NO_2^- does not absorb between 200 and 300 nm. Since the luminescence

lifetime of the sensor decreased in the presence of NO_2^-, the quenching effect of NO_2^- could be due to the collisional deactivation of the excited state of the probe (dynamic quenching).

The signal enhancement observed in the presence of CO_3^{2-}, Cl^- and F^- can be attributed to their chemical affinity for the CTAB receptors and/or their chemical interaction with the coordination sphere of lanthanide ion. Similar to the phosphate ions, the interaction of CO_3^{2-}, Cl^- and F^- with CTAB appears to displace a significant portion of $[Tb\text{-}EDTA]^{-1}$ to the bulk of the solution where FRET does not longer occur. The longer luminescence lifetimes of the probe in the presence of $CO_3^{2-}$and Cl^- are probably due to the replacement of water molecules in the inner coordination sphere of Tb^{3+}. These heavier oscillators might decrease the vibrational deactivation of Tb^{3+} and enhance the luminescence signal of the probe. Since the luminescence lifetime in the presence of F^- is statistically equivalent to the lifetime of the probe in the absence of this ion, the signal enhancement due to the presence of F^- should be solely attributed to the release of $[Tb\text{-}EDTA]^{-1}$ into the bulk of the sensing solution.

Fig. 3A shows a calibration curve built in HEPES (pH ≈7.5) with external standards containing different concentrations of phosphate ions and the synthetic mixture in Table 1. Linear regression via the least squares method provided a linear dynamic range (correlation coefficient =0.9947) ranging from 6.3×10^{-6} mol L^{-1} to 7.5×10^{-4} mol L^{-1}. The limit of detection (1.8 μmol L^{-1}) was calculated as 3 s_C/m; where s_C is the standard deviation of 16 control measurements and m is the slope of the best linear fit ($y=3\cdot10^7x+7215.3$).

The well-behaved single exponential luminescence decay observed in the absence (see Fig. 3B) and the presence of the synthetic mixture indicate one predominant emitting species within the entire linear dynamic range of the calibration curve. Since the luminescence lifetime of the probe (1060.3 ± 33.9 μsec) remained statistically the same in all measured solutions, the major emitting species most likely refers to $[Tb\text{-}EDTA]^{-1}$. The lifetime effects observed with individual species appear to cancel out with their simultaneous presence in a synthetic mixture.

3.6. Urine analysis

Urine samples from healthy, non-smoking volunteers were used for this study. A representative clinical sample was obtained by mixing all the samples immediately after collection. The representative mixture was kept refrigerated at 4 °C until further use. In order to remove particulate matter and obtain optically transparent solutions for luminescence measurements, the urine sample required a two-cycle filtration step prior to phosphate determination. Quantitative analysis was performed via the multiple standard addition method with a 0.025 mol L^{-1} PO_4^{3-} standard solution prepared in HEPES buffer (pH≈7.5). Microliter standard additions were made to 1 mL of filtered urine and 8 μL of pre-treated urine were added to the sensing solution consisting of 350 μL of Au NPs-CTAB (optical density =0.74 OD) and 150 μL of 10^{-5} mol L^{-1} $[Tb\text{-}EDTA]^{-1}$. Luminescence measurements were carried out after 10 min of mechanical shaking using the instrumental parameters described previously. A linear correlation was observed between the luminescence signal (Y) and the concentration of phosphate (X) in the optical sample. Fitting of the experimental data via the least squares method [30] provided the following linear equation: $Y=3\cdot10^7X+1804.5$. The concentration of phosphate found in the urine sample (399 ± 24 mgL^{-1}) was within the reported values of urine samples collected from healthy individuals [7–12]. Monitoring of the luminescence lifetime of $[Tb\text{-}EDTA]^{-1}$ within the entire concentration range of standard additions confirmed the lack of chemical interference with the lanthanide ion.

4. Conclusion

A novel sensor for the determination of inorganic phosphate in urine samples was developed based on the FRET that occurs between $[Tb\text{-}EDTA]^{-1}$ (donor) and Au NPs-CTAB (acceptor). The luminescence lifetime of $[Tb\text{-}EDTA]^{-1}$ makes possible to interrogate the sensor for potential chemical interference. No interference from concomitant species such as creatinine, urea, NO_3^-, NO_2^-, OH^-, CO_3^{-2}, Cl^-, F^-, CH_3COO^- and I^- was observed at the concentrations normally found in urine samples. The high selectivity of the proposed sensor is attributed to the chemical affinity between HPO_4^{2-} ions and the CTAB receptors on the surface of Au NPs. Their strong interaction leads to a simple assay with minimum sample preparation steps. The LOD (3.8 μmol L^{-1}) is within the concentration range of sensing approaches reported previously [6–12]. The simplicity of analysis and the competitive LOD provide a well-suited approach for routine monitoring of phosphate ions in numerous urine samples.

References

[1] C.M. Porth, Pathophysiology: Concepts of Altered Health States, eighth ed., Lippincot-raven, Philadelphia, 1998.
[2] G.C. Schussler, M. Verso, T. Nemoto, Phosphatemia in hypercalcemic breast cancer pantients, J. Clin. Endocrinol. Metab. 35 (1972) 497–504.
[3] S. Norenstedt, F. Granath, A. Ekbom, Breast cancer associated with primary hyperparathyroidism: a nested case control study, Epidemiology 3 (2011) 103–106.
[4] J.M. Sharretts, E. Kebebew, E.F. Simonds, Parathyroid cancer, Semin. Oncol. 37 (6) (2010) 580–590.
[5] J.A. Daly, G. Ertingshausen, Direct method for determining inorganic phosphate in serum with "CentrifiChem", Clin. Chem. 18 (3) (1972) 263–265.
[6] A.T. Law al, S.B. Adeloju, Progress and recent advances in phosphate sensors: a review, Talanta 114 (2013) 191–203.
[7] D.G. Themelis, A. Economou, A. Tsiomlektsis, P.D. Tzanavaras, Direct determination of phosphate in urine by sequential-injection analysis with single on-line dilution-calibration method and photometric detection, Anal. Biochem. 330 (2) (2004) 193–198.
[8] E. Lozano-Chaves, M.P. Hernández-Artiga, A. Muñoz-Leyva, Spectrophotometric phosphate determination in urine by ligand exchange extraction, Microchim. Acta 116 (1994) 91–99.
[9] A. Classen, W.D. Miersch, A. Hesse, Simultaneous determination of urinary phosphate and sulphate by ion-chromatography, J. Clin. Chem. Clin. Biochem. 28 (1990) 91–94.
[10] U.K. Abcam, Phosphate Assay Kit (Fluorometric). ⟨http://www.abcam.com/phosphate-assay-kit-fluorometric-ab102508-references.html⟩(accessed 3.16.16), 2016.
[11] L. Gilbert, A.T.A. Jenkins, S. Browning, J.P. Hart, Development of an amperometric assay for phosphate ions in urine based on a chemically modified screen-printed carbon electrode, Anal. Biochem. 393 (2) (2009) 242–247.
[12] J. Hatai, S. Pal, S. Bandyopadhyay, An inorganic phosphate (Pi) sensor triggers 'turn-on' fluorescence response by removal of a Cu^{2+} ion from a Cu^{2+}-ligand sensor: determination of Pi in biological samples, Tetrahedron Lett. 53 (33) (2012) 4357–4360.
[13] G. Mathis, Probing molecular interactions with homogeneous techniques based on rare earth cryptates and fluorescence energy transfer, Clin. Chem. 41 (9) (1995) 1391–1397.
[14] R.M. Clegg, Fluorescence resonance energy transfer and nucleic acids, Methods Enzym. 211 (1992) 353–388.
[15] P.R. Selvin, The renaissance of fluorescence resonance energy transfer, Nat. Struct. Biol. 7 (9) (2000) 730–734.
[16] R. Barbieri, I. Bertini, G. Cavallaro, Ym Lee, C. Luchinat, A. Rosato, Paramagnetically induced residual dipolar couplings for solution structure determination of lanthanide binding proteins, J. Am. Chem. Soc. 124 (19) (2002) 5581–5587.
[17] M.P. Bemquerer, C. Bloch, H.F. Brito, E.E.S. Teotonio, M.T.M. Miranda, Luminescence investigation of binding Eu and Tb ions with the synthetic peptides derived from the plant thionins, J. Inorg. Biochem. 9 (2002) 363–370.
[18] K.J. Franz, M. Nitz, B. Imperiali, Lanthan.-Bind. Tags. versatile Protein coexpression probes. Chem. Bio. Chem. 4 (2003) 265–271.
[19] P.R. Selvin, Lanthanide-based resonance energy transfer, IEEE J. Sel. Top. Quantum Electron. Lasers Biol. 2 (4) (1996) 1077–1087.
[20] M. Santos, B.C. Roy, H.C. Goicoechea, A.D. Campiglia, S. Mallik, An investigation of the analytical potential of polymerized liposomes bound to lanthanide Ions for protein analysis, J. Am. Chem. Soc. 126 (2004) 10738–10745.
[21] H.C. Goicoechea, M. Santos, B.C. Roy, A.D. Campiglia, S. Mallik, Evaluation of two lanthanide complexes for qualitiative and quantitative analysis of target proteins via partial least squares analysis, Anal. Biochem. 336 (2005) 64–71.
[22] M. Santos, S. Nadi, H.C. Goicoechea, M.K. Haldar, A.D. Campiglia, S. Mallik, Artificial neural networks for qualitative and quantitative analysis of target proteins with polymerized liposome vesicles, Anal. Biochem. 361 (2007) 109–119.
[23] M. Swierczewska, S. Lee, X. Chen, The design and application of fluorophore-gold nanoparticle activatable probes, Phys. Chem. Chem. Phys. 13 (21) (2011) 9929–9941.

[24] M.C. Daniel, D. Astruc, Gold nanoparticles: assembly, supramolecular chemistry, quantum size-related properties, and applications toward biology, catalysis, and nanotechnology, Chem. Rev. 104 (1) (2004) 293–346.
[25] J. Homola, Surface plasmon resonance sensors for detection of chemical and biological species, Chem. Rev. 108 (2) (2008) 462–493.
[26] B. Nikoobakht, M.A. El-Sayed, Preparation and growth mechanism of gold nanorods (NRs) using seed-mediated growth method, Chem. Mater. 15 (10) (2003) 1957–1962.
[28] J.K. Prashant, K.S. Lee, I.H. El-Sayed, M.A. El-Sayed, Calculated absorption and scattering properties of gold nanoparticles of different size, shape, and composition: application in biological Imaging and biomedicine, J. Phys. Chem. B 110 (14) (2006) 7238–7248.
[29] W.D. Horrocks Jr., D.R. Sudnick, Lanthanide ion luminescence probes of the structure of biological macromolecules, Acc. Chem. Res. 14 (1981) 384–392.
[30] J.N. Miller, J.C. Miller, Statistics and Chemometrics for Analytical Chemistry, fourth ed., Pearson, New York, 2000.
[31] F.P. Underhill, A Manual of Selected Biochemical Methods as Applied to UrineBlood, and Gastric Analysis, John Wiley, New York, 1921.
[32] E. Marcos, N.P. Wiklund, Nitrite and Nitrate measurement in human urine by capillary electrophoresis, Methods Mol. Biol. 279 (2004) 21–34.
[33] S. Kage, K. Kudo, H. Ikeda, N. Ikeda, Simultaneous determination of formate and acetate in whole blood and urine from humans using gas chromatography-mass spectrometry, J. Chromatogr. B. Anal. Technol. Biomed. Life Sci. 805 (2004) 113–117.
[34] K.H. Kang, W.X. Huang, Y.H. Su, R.Z. Hu, Simultaneous determination of fluorine and iodine by in urine by ion chromatography with electrochemical pretreatment 20 (2009) 1483–1486.
[35] NASA, Composition and concentrative properties of human urine. ⟨https://ntrs.nasa.gov/archive/nasa/casi.ntrs.nasa.gov/19710023044.pdf⟩, 1971 (accessed 11.01.16).
[36] Healthline, Urine pH levels test. ⟨http://www.healthline.com/health/urine-ph⟩, 2016 (accessed 11.01.16).